Robust Terrain Navigation with the Correlation Method for High Position Accuracy

Ingemar Nygren, Magnus Jansson
inygren@s3.kth.se, magnus.jansson@s3.kth.se
Department of Signals, Sensors and Systems
Royal Institute of Technology (KTH), Sweden

Abstract - **The purpose of this paper is to describe the correlation method for determining the position of an autonomous underwater vehicle (AUV) in shallow waters. The method is conceptually simple. It involves measuring the seabed topography with a few sonar pings over a limited area by an ordinary bathymetric multibeam sonar. These measurements are then correlated with existing underwater maps. The position estimate from the correlation method can often be used as it is or fused by a linear Kalman filter with almost optimal performance. The paper also shows results from a sea-trial with the Reson SeaBat 8001 multibeam bathymetric sonar. The achieved 1 σ - circular accuracy is 0.3 - 0.4 meter in the north of the Baltic Sea.**

I. INTRODUCTION

In many autonomous underwater vehicle (AUV) applications, there is a need to accurately determine the AUV's position in relation to the underlying bottom structures or in relation to the coordinates on a map in an effective way. An often proposed solution to the positioning problem is to use a method similar to the terrain navigation method used to guide cruise missiles [1], [2]. See Figure 1. The measurements are integrated with an inertial navigation system (INS) by an extended Kalman filter (EKF) [3] or by a Bayesian recursive filter implemented as a mass point filter or a particle filter [4]. However, these methods are not particularly accurate or energy-effective since the sonar has to work continuously with a power drain almost as high as for propulsion. This is an important point for battery operated vehicles. The computational cost for the mass point and the particle filter, which are optimal filters, is high compared to that of the sub-optimal EKF filter. Furthermore, underwater maps have to be available for the whole area over which the AUV operates.

This paper describes a different method [5], called the correlation method, with high accuracy and a filter with almost optimal performance. Figure 2 illustrates how the bottom topography is measured by a 3D bathymetric sonar. The correlation method has successfully been tested in a non-recursive mode but can of course also be used in a recursive mode. This will greatly improve the performance in very flat areas. The sampling frequency of the bottom topography can be very infrequent and the position can often be determined by only a single sonar ping. The method is more robust than the conventional terrain navigation methods using only one measurement beam. The method does only need maps where the sampling of the bottom topography takes place and not over the whole area of operation. This is a great advantage since high quality underwater maps are rare. Typically, way-

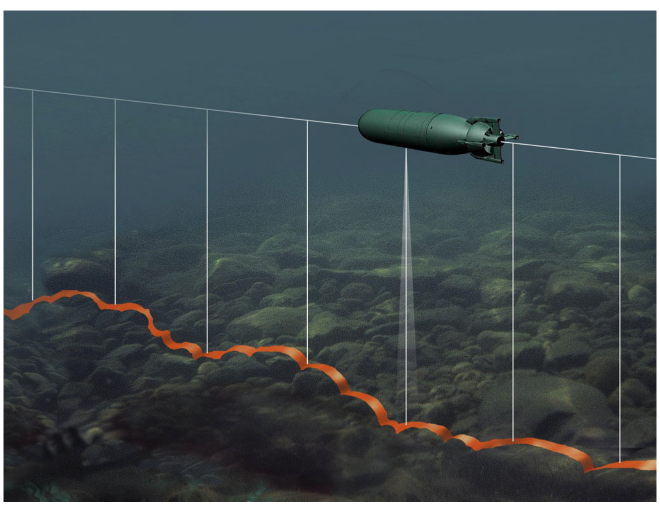

Fig.1. Terrain navigation according to the cruise missile principle. The vehicle is measuring the depth by one sonar beam at each sampling event. Likely positions are positions in the map with the same depth.

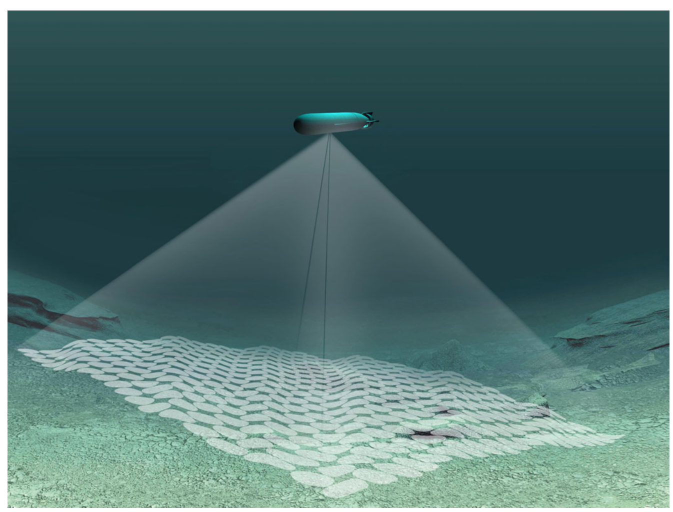

Fig.2. The bottom topography measurement with the correlation method. The vehicle is measuring the bottom topography by several sonar beams. Likely positions are positions with the same bottom topography.

points are placed at mapped areas and the travelling time between way-points can be hours.

The aim with the current paper is to formulate a linear optimal Kalman filter for terrain navigation instead of the usual sub-optimal extended Kalman filter.

The paper begins in Section II by comparing recursive terrain navigation in two cases. The first case uses one beam to measure the distance to the bottom (cf. Figure 1). The second case uses several beams for the measurement (cf. Figure 2). In Section II the estimation problem is looked upon from a Bayesian viewpoint. This reveals the great difference between measuring with one beam and measuring with several beams. Some figures showing this are given and the section ends with an explanation of the cause for that.

In order to formulate a linear Kalman filter the position error covariance has to be known. The asymptotic properties of the maximum likelihood (ML) estimator will provide this information. Therefore Section III discusses ML estimation in this respect.

Section IV discusses the formulation of the linear Kalman filter. Section V describes the hardware solution that has been used for calculating the likelihood function for the ML-estimator. Section VI gives results from sea-trials and Section VII concludes the article.

II. BAYESIAN RECURSIVE ESTIMATION

Figure 2 shows an underwater vehicle that measures the bottom topography over a large bottom area with a large number of sonar beams at each sampling event. The assumption for the evolution of the state space is

$$\mathbf{x}_{t+1} = \mathbf{x}_t + \mathbf{u}_t + \mathbf{v}_t \qquad t = 1,2,3... \tag{1}$$

$$\mathbb{Y}_t = \mathbb{H}(\mathbf{x}_t) + \mathbb{E}_t \tag{2}$$

where $\mathbf{x}_t$ is the position in the horizontal plane at time t and $\mathbf{u}_t$ - the distance between the positions - is provided by the INS system. The measured depths to the bottom are collected in the matrix $\mathbb{Y}_t$ and the matrix $\mathbb{H}(\mathbf{x}_t)$ collects the depths according to the map if we are in position $\mathbf{x}_t$. The error in the INS system is $\mathbf{v}_t$ and $\mathbf{E}_t$ is the error in the depth measurement. The number of measurement points (sonar beams) is N. In order to simplify the discussion we vectorize (2)

$$\mathbf{y}_t = \mathbf{h}(\mathbf{x}_t) + \mathbf{e}_t \tag{2b}$$

and we will assume that the measurement errors are independent white Gaussian sequences.

The Bayesian way of looking at the estimation problem can be quite illustrative. It is well known that the optimal estimate in the linear and nonlinear cases is given by the conditional mean. The conditional probability density function (PDF) is given by

$$p(\mathbf{x}\,|\,\mathbf{y}) = \frac{p(\mathbf{y}\,|\,\mathbf{x})p(\mathbf{x})}{p(\mathbf{y})} = \frac{L(\mathbf{y}\,|\,\mathbf{x})p(\mathbf{x})}{\int_{R^2} L(\mathbf{y}\,|\,\mathbf{x})p(\mathbf{x})d\mathbf{x}} \tag{3}$$

where $\int_{R^2} L(\mathbf{y}\,|\,\mathbf{x})p(\mathbf{x})d\mathbf{x}$ can be interpreted as a normalizing constant. We call $L(\mathbf{y}\,|\,\mathbf{x}) = p(\mathbf{y}\,|\,\mathbf{x})$ the likelihood function and refer to $p(\mathbf{x}\,|\,\mathbf{y})$ as the posterior PDF, while $p(\mathbf{x})$ is referred to as the prior PDF.

The recursive procedure means that we will start from a given prior PDF that we will propagate according to the movement of the vehicle and the uncertainty of the movement. The movement can, for example, be determined from an INS system that has a specified uncertainty. We can denote the propagated, but not measurement updated, PDF as $p^-(\mathbf{x})$. The next step in the recursive procedure is to do the measurement update of $p^-(\mathbf{x})$ by multiplication of $p^-(\mathbf{x})$ and $L(\mathbf{y}\,|\,\mathbf{x})$ in order to arrive at the posterior PDF . In the following we will look at this in some more details.

A. Propagation of the PDF for the vehicle position

The first equation (1) describes how the position changes between two sampling events. Figure 3 illustrates this. The left PDF (prior PDF) has a bearing upon the vehicle's position at sampling time t and the black pile is the relative frequency of the number of realizations which have ended in point $\mathbf{x}_t$, i.e. $p(\mathbf{x}_t\,|\,\mathbf{Y}_t)$. The notation $p(\cdot\,|\,\mathbf{Y}_t)$ indicates that the PDF is based on all measurements up to and including the measurement at time t. The realizations are moved the distance $\mathbf{u}_t$ but due to the uncertainty $\mathbf{v}_t$ we will have a spread in the new position. We multiply this new PDF - the small one in the figure - by the relative frequency $p(\mathbf{x}_t\,|\,\mathbf{Y}_t)$ and total the contributions of all points in the left PDF by an integral to get the position PDF at time t+1. We can express the propagation as

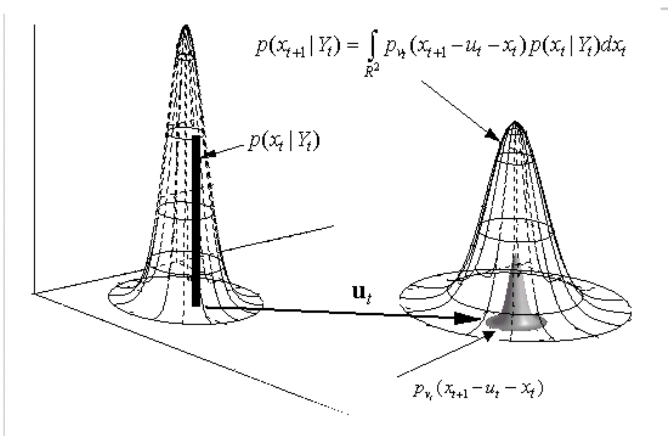

Fig.3. Propagation of the PDF for the vehicle position.

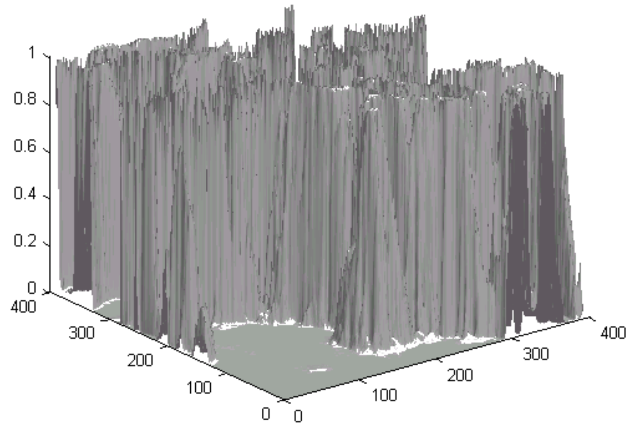

Fig. 4. The non-normalized likelihood function when using one measurement beam. Map area 4 km x 4 km.

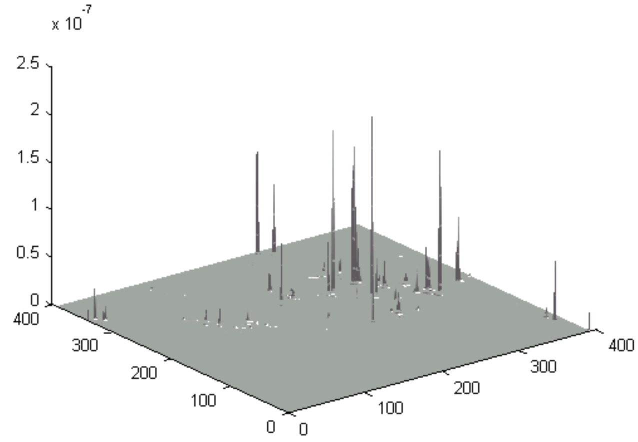

Fig. 5. The non-normalized likelihood function when using 9 x 9 measurement beams. Map area 4 km x 4 km.

$$p(\mathbf{x}_{t+1} \mid \mathbf{Y}_t) = \int_{R^2} p_{\mathbf{v}_t}(\mathbf{x}_{t+1} - \mathbf{u}_t - \mathbf{x}_t)\, p(\mathbf{x}_t \mid \mathbf{Y}_t) d\mathbf{x}_t \tag{4}$$

where $p_{\mathbf{v}_t}(\cdot)$ is the PDF for the error term $\mathbf{v}_t$.

B. The measurement update

The measurement update is made according to (2b). We assume the error in the depth measurement to be Gaussian and independent. Therefore

$$L(\mathbf{y}_t|\mathbf{x}_t) = \frac{1}{\sqrt{(2\pi)^N \det(\mathbf{C}_e)}} e^{-\frac{1}{2}(\mathbf{y}_t - \mathbf{h}(\mathbf{x}_t))^T \mathbf{C}_e^{-1}(\mathbf{y}_t - \mathbf{h}(\mathbf{x}_t))} \tag{5}$$

where $\mathbf{C}_e$ is the measurement error covariance matrix. The function $L(\mathbf{y}_t \mid \mathbf{x}_t)$ is our likelihood function since, for a given position $\mathbf{x}_t$, it gives the likelihood of having the measurement value $\mathbf{y}_t$. The assumption that the error of different beams are uncorrelated makes the correlation matrix $\mathbf{C}_e$ diagonal and equal to $\sigma_e^2\mathbf{I}$. Therefore the likelihood function will be

$$L(\mathbf{y}_t|\mathbf{x}_t) = \frac{1}{\sqrt{(2\pi\sigma_e^2)^N}} e^{-\frac{1}{2\sigma_e^2}\sum_{k=1}^{N}(y_{t,k} - h_k(\mathbf{x}_t))^2} \tag{6}$$

where $y_{t,k}$ and $h_k(\mathbf{x}_t)$ are the kth components of the vectors $\mathbf{y}_t$, $\mathbf{h}(\mathbf{x}_t)$ respectively.

Figure 4 shows the non-normalized likelihood function for a measurement with only one beam, which is the usual way that the measurement is done in terrain navigation. Figure 5 shows the likelihood function corresponding to a measurement with 9 x 9 beams. The size of the map is 4 x 4 km in both cases. It can be seen from the figures that using a large number of beams drastically reduces the number of likely positions.

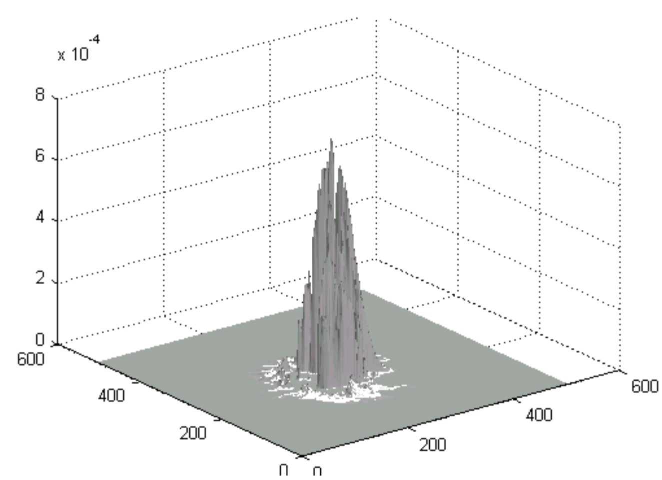

Fig. 6. The non-normalized measurement updated prior for one measurement beam. Map area 4 km x 4 km.

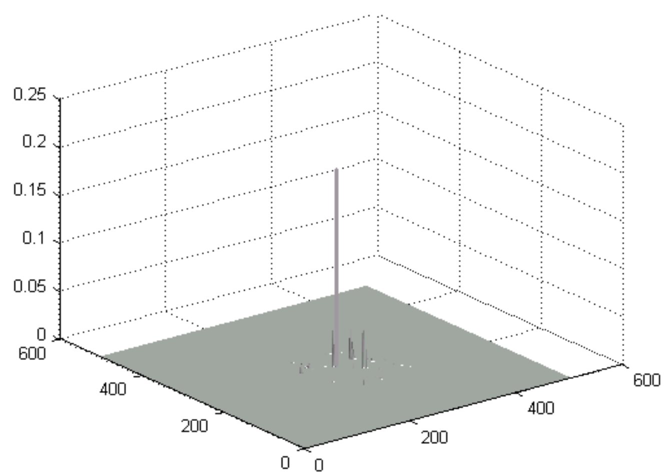

Fig. 7. The non-normalized measurement updated prior for 9 x 9 measurement beams. Map area 4 km x 4 km.

The next step in the recursion is to fuse the likelihood function for the measurement with the propagated PDF of the position. The Figures 6 and 7 show the non-normalized measurement updated PDF, the posterior PDF. The equation for the fusion before normalization of the posterior is

$$p(\mathbf{x}_{t+1} \mid \mathbf{Y}_{t+1}) \sim L(\mathbf{y}_{t+1} \mid \mathbf{x}_{t+1}) p(\mathbf{x}_{t+1} \mid \mathbf{Y}_t) \tag{8}$$

A comparison between Figure 6 and 7 shows, as expected, that the variance is much smaller when many beams are used in the measurement.

If the time between the measurements is large, the variance in the propagated PDF, $p^-(\mathbf{x})$, may increase such that it will not noticeably improve the estimation of the position based on the likelihood function. Hence, when the prior PDF has a large variance the estimation problem becomes a ML estimation problem.

III. MAXIMUM LIKELIHOOD ESTIMATION

We know from the theory of ML estimation that, under weak assumptions, the ML-estimate, [6] [7]

- is asymptotically unbiased
- asymptotically reaches the Cramér-Rao lower bound
- is asymptotically Gaussian distributed

The asymptotic covariance of the ML-estimate $\hat{\mathbf{x}}(\mathbf{y})$ can therefore be expressed as

$$\mathbf{R} = E\{[\hat{\mathbf{x}}(\mathbf{y}) - \mathbf{x}]^2\} = \mathbf{J}^{-1} \tag{9}$$

where $\mathbf{J}$ is Fisher's information matrix

$$\mathbf{J} = -E\{\frac{\partial^2[\ln p(\mathbf{y} \mid \mathbf{x})]}{\partial\mathbf{x}\partial\mathbf{x}^T}\} \tag{10}$$

We have

$$\mathbf{R} = \sigma_e^2 \begin{bmatrix} \sum_{i=1}^{N} \frac{\partial^2 h_i}{\partial x_1^2} & \sum_{i=1}^{N} \frac{\partial^2 h_i}{\partial x_1 \partial x_2} \\ \sum_{i=1}^{N} \frac{\partial^2 h_i}{\partial x_2 \partial x_1} & \sum_{i=1}^{N} \frac{\partial^2 h_i}{\partial x_2^2} \end{bmatrix}^{-1} \tag{11}$$

where index *i* refers to the derivative at beam *i* and x_1, x_2 refer to the east and north directions, respectively.

The variance in the position estimate can thus be calculated in real time or in advance from the underwater map if so is wanted. Figure 8 shows the convergence of the Cramér-Rao lower bound given by (11) for way-point three in the October 2002 sea-trial described in section VI. Normally we use more than 150 measurement beams depending on the actual sonar. In the sea-trial we used 400 beams and from Figure 8 we conclude we are close to the asymptotic value of the covariance matrix.

Of great interest in our case is the convergence of the normalized likelihood function towards the Gaussian PDF. Even if the exponent in our likelihood function (6) is quadratic in $h(\mathbf{x})$ we expect it to be close to a Gaussian function with respect to $\mathbf{x}$. Figure 9 shows a comparison between the likelihood function and the Gaussian curve for real measurements and real maps with 400 measuring beams assembled from 5 beam planes. Data is from the way-point three in the sea trial, Figure 19. As can be seen the likelihood function is approximately Gaussian.

Figure 10 shows the likelihood functions for different numbers of measuring beams. In the legend box, for example,

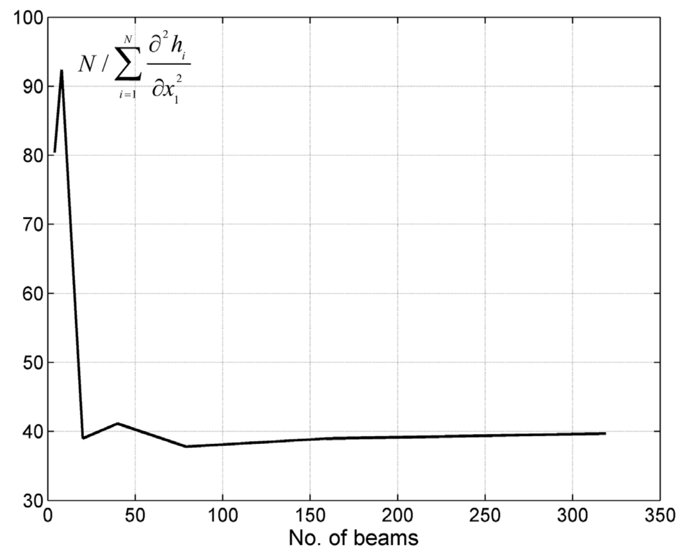

Fig. 8. The convergence of the Cramér-Rao bound as a function of the number of measurement beams. Data from WP3 in the October 2002 sea-trial.

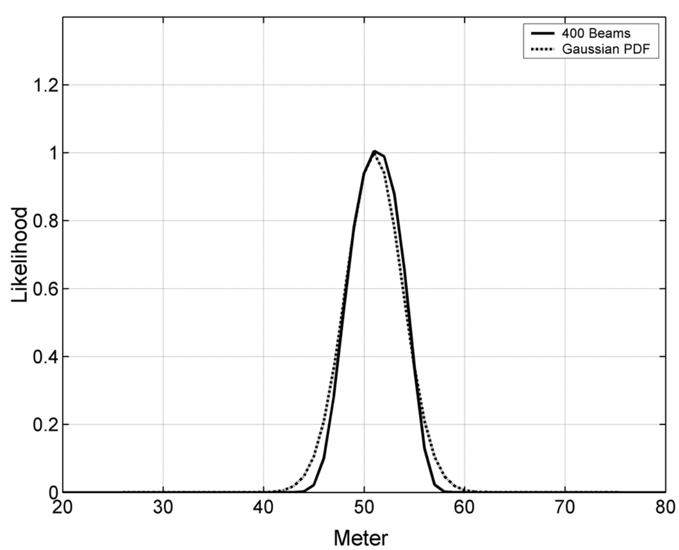

Fig. 9. Comparison between the likelihood function and the Gaussian PDF. Data from WP3 in the October 2002 sea-trial.

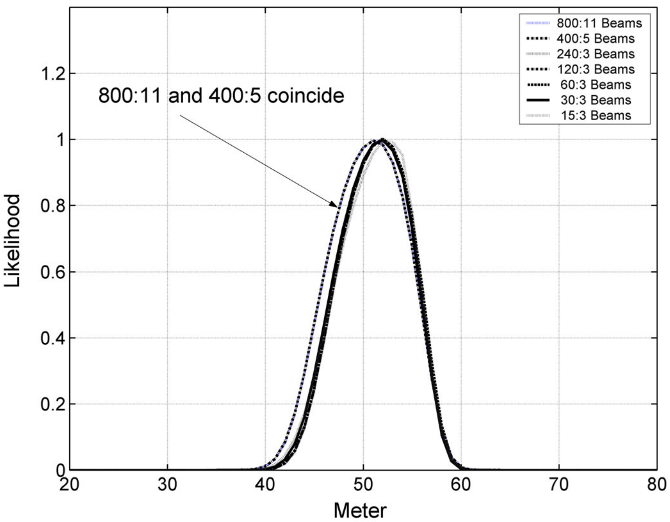

Fig. 10. Comparison between the likelihood functions for different numbers of measurement beams. The exponent in the likelihood function (6) has been normalized by $1/N$ to allow a comparison.

400:5 means that the 3D sonar measurement is composed from 5 beam planes (pings).

Call the covariances for the posterior PDF, prior PDF and the likelihood function for $\mathbf{P}, \mathbf{P}^-, \mathbf{P}_L$, respectively. It is reasonable to assume, due to the central limit theorem, that the likelihood PDF is asymptotically Gaussian. Fusing the prior PDF and the likelihood PDF, according to (8) then gives

$$\mathbf{P}^{-1} = (\mathbf{P}^-)^{-1} + \mathbf{P}_L^{-1} \ . \tag{12}$$

Now, if the prior PDF is non-informative it follows that $\mathbf{P} = \mathbf{P}_L$ but this is also, in our case, the error covariance for the maximum likelihood estimate, **R**, since the prior was non-informative. Since the maximum likelihood PDF is independent of the prior PDF we then have

$$\mathbf{P} = \mathbf{R} = \mathbf{P}_L \tag{13}$$

Since the Gaussian PDF is completly defined by the first and second moments it also follows that the likelihood PDF and the PDF for the ML-estimate are the same. We conclude that assuming the normalized likelihood function to be Gaussian and with a covariance according to (11) will only amount to a small approximation.

IV. THE LINEAR KALMAN FILTER

In order to formulate the linear Kalman filter we redefine our measurement equation (2b)

$$\mathbf{x}_{t+1} = \mathbf{x}_t + \mathbf{u}_t + \mathbf{v}_t \qquad t = 1, 2, 3...$$

$$\mathbf{z}_t = \mathbf{x}_t + \mathbf{w}_t \tag{14}$$

Here $\mathbf{z}_t$ is our measured position given by the correlation between the sonar map and the underwater map, the ML-estimate, and the error term $\mathbf{w}_t$ is assumed to be a white sequence with zero mean. The covariance of $\mathbf{w}_t$ is given by (11).

In the following, as before, the superscript − means the quantity before measurement update. The INS-system is assumed to be reset after each determination of the position. The prior estimated position, $\mathbf{x}_t^-$, the propagation step in the Kalman recursive algorithm, will therefore directly be given by the INS-system [8].

For the linear Kalman filter we assume the following covariance matrix for the prior PDF

$$\mathbf{Q}_t = E\{\mathbf{v}_t \mathbf{v}_t^T\} \tag{15}$$

Due to irregular sampling it will be time dependent [8]. Our measurement updated position will be

$$\hat{\mathbf{x}}_t = \mathbf{x}_t^- + \mathbf{K}_t(\mathbf{z}_t - \mathbf{x}_t^-) \tag{16}$$

where the Kalman gain is

$$\mathbf{K}_t = \mathbf{P}_t^- \left(\mathbf{P}_t^- + \mathbf{R}_t\right)^{-1} \tag{17}$$

and the covariance of the propagated old posterior position estimate

$$\mathbf{P}_t^- = \mathbf{P}_{t-1} + \mathbf{Q}_t \tag{18}$$

The covariance for the measurement updated position is given by (12)

$$\mathbf{P}^{-1} = (\mathbf{P}^-)^{-1} + \mathbf{P}_L^{-1} \ .$$

Note that, when we have a low informative prior position PDF we have $\mathbf{P}_t \approx \mathbf{R}_t$, $\mathbf{K}_t = \mathbf{I}$, $\hat{\mathbf{x}}_t = \mathbf{z}_t$.

Since the normalized likelihood function is very close to the Gaussian PDF, the filter will be almost optimal. It can also be worth noting that a larger number of measurement beams makes the propagation stage more robust to modelling errors in the propagation. This can be seen from Figure 6. An error in the propagation of the prior PDF will select a wrong part of the likelihood function for calculating the position estimate and the posterior PDF's covariance. As can be seen from Figure 7 an error in the propagation will have a very low influence on the position estimate of the position when we have a larger number of measurement beams.

An important side effect of the linearization is that the presented method easily can be applied to a more general process model [9]

$$\mathbf{x}_{t+1} = \mathbf{F}_t \mathbf{x}_t + \mathbf{G}_t \mathbf{u}_t + \mathbf{\Gamma}_t \mathbf{v}_t \tag{19}$$

with the state vector extended to include the state variables of the INS-system and thus avoiding the complication with Rao-Blackwellization as in the particle filter [9],[10].

V. THE HARDWARE CORRELATOR

The described principle to achieve nearly optimal performance implies that much of the computational work in the filter is shifted from propagation and fusion to the computation of the likelihood function. However, since the likelihood function is easy to compute without any computational problems this is

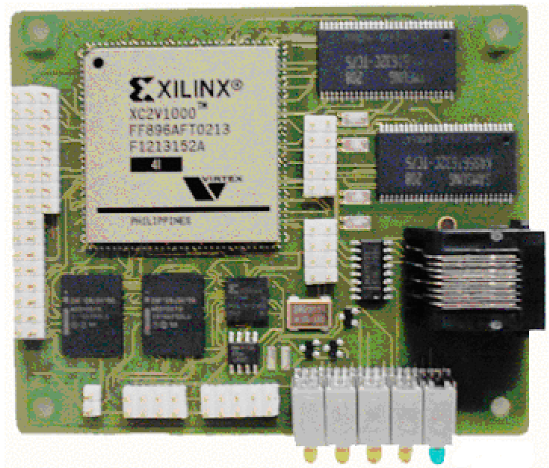

Fig. 11. The prototype board for the hardware correlator. Physical size is 90 mm x 70 mm.

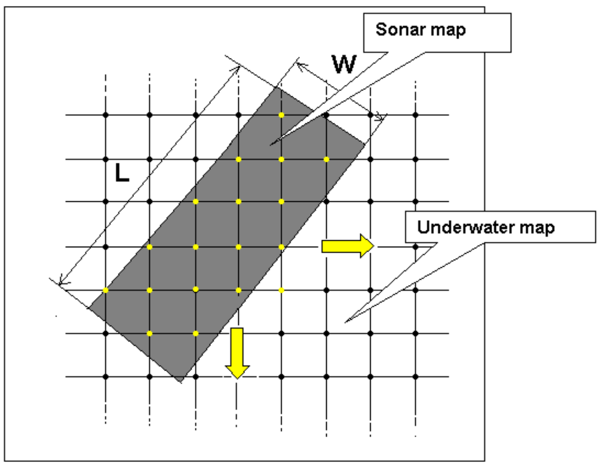

Fig. 12. The principle for calculating the correlation sum in the hardware correlator.

not a drawback. Especially since the computations are easy to mechanize.

A hardware device calculating the likelihood function has therefore been built based on a field programmable gate array (FPGA). See Figure 11. The FPGA is a highly parallel fast computing device.
The physical size of the computer board is 90 mm by 70 mm. It computes the likelihood function for 100 beams on a map with 501 by 501 nodes in 266 ms [11]. The latest design will do the same calculations in 30 ms.

The principle for the calculations can be seen from Figure 12 where the gridded sonar measurement is compared, in steps, with all nodes in the underwater map. The position where the likelihood function (6) takes its highest value is considered to be the position according to the measurement, the ML-estimate. The error covariance is calculated for that position according to (11).

VI. SEA TRIALS

A number of sea-trials have been conducted to verify the theoretical results. The magnitude of the position error of course depends on the flatness of the sea bottom. In the north part of the Baltic Sea we have achieved in simulation 1 σ - circular position errors, due to only the measurement noise, in the 0.3 – 0.4 meter range. It should, however, be noted that there are several other sources of position errors that can be of greater concern than the position error due to measurement noise.

Such errors may result from misalignment of the sonar equipment, incomplete calibration, or incomplete corrections for the vehicle's motion in terms of roll, pitch and heave. Other types of errors are vertical and horizontal map errors and DGPS errors if DGPS is used as a position reference.

In October 2002 we conducted a sea trial in the Stockholm archipelago sailing a distance of about 60 kilometers with eight way-points. We tried to determine our position at each way-point by means of the correlation method using data obtained with the Reson 8101 bathymetric sonar. We also collected sediment profiles and conventional side-scan data. The Reson bathymetric sonar was attached to a pole that was lowered through the moon pool at the stearn of the ship. Side-scan data were also collected with the Reson sonar but the main source of side-scan data was the fish-mounted Datatronic SIS-1000, 100-110 kHz chirp sonar and the Klein CW- puls 50 kHz sonar. We used an Edo Western 515-A, 3.5 kHz sediment profiler with 19 degrees beamwidth for collecting sediment data.

Figures 13 - 18 show the likelihood functions for six positionings along the track in Figure 20. Ping 500 is the position far to the left in the figure. There are 200 pings between the positionings, corresponding to approximately 80 meters between the positions. The size of the correlation area is approximately 50 by 102 meters.

As can be seen from the figures the positioning is excellent except for ping 700 and to a certain degree also for ping 500. The position errors for these pings appear in Table I. The position reference used was an FM DGPS with corrections update every two seconds.

Three error values are given for ping 700. The first '-' indicates that the position was not found as can be seen in Figure 14. The second figure corresponds to an increase in the measurement area to approximately 97 x 102 meters. Doing so the bottom topography will be more unique. The third values were obtained when the measurement area was increased to 121 x 102 meters. The corresponding likelihood functions appear in Figures 21 and 22. Figures 21 and 22 emphasize the importance of having a large correlation area.

As can be seen from Table I we have a systematic position error if our position reference is a map. This is due to a horizontal error of the nodes in the map of about 12 meters along the track. A simple correction for this would be to reduce the error values in Table I by the mean of the error. The position errors would then be as in Table II.

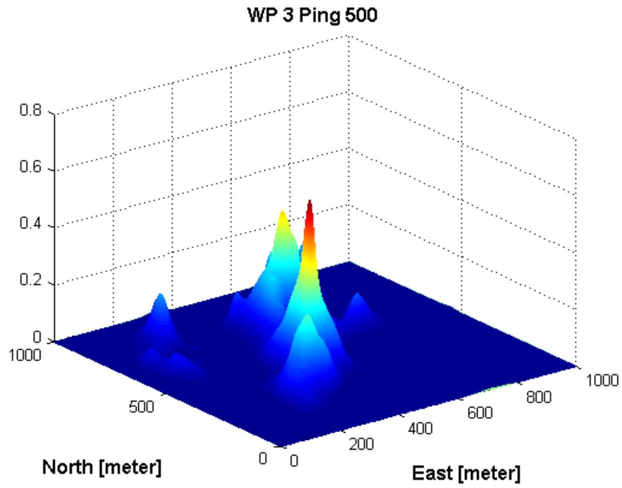

Fig. 13. Likelihood function for ping 500.

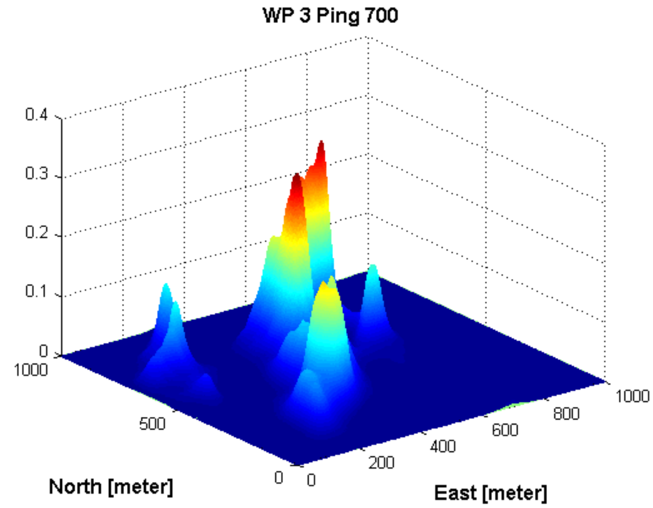

Fig. 14. Likelihood function for ping 700.

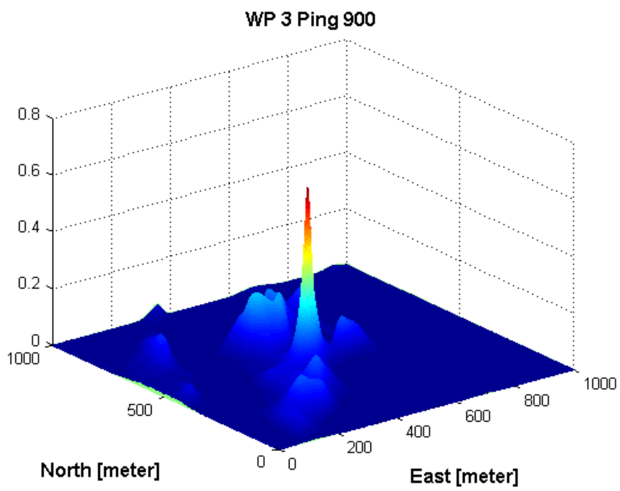

Fig. 15. Likelihood function for ping 900.

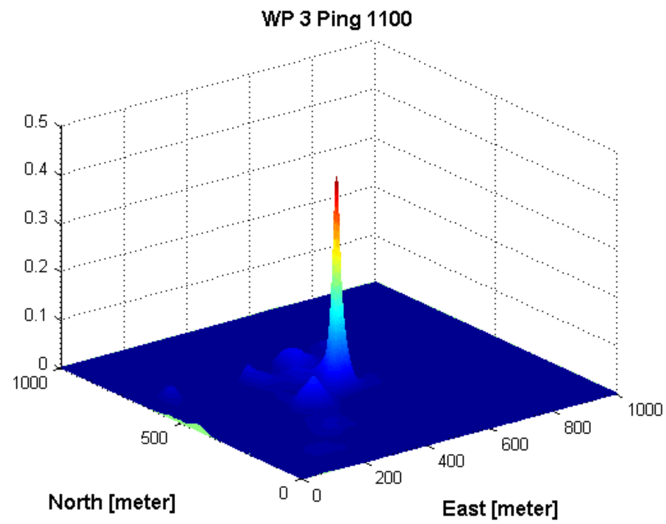

Fig. 16. Likelihood function for ping 1100.

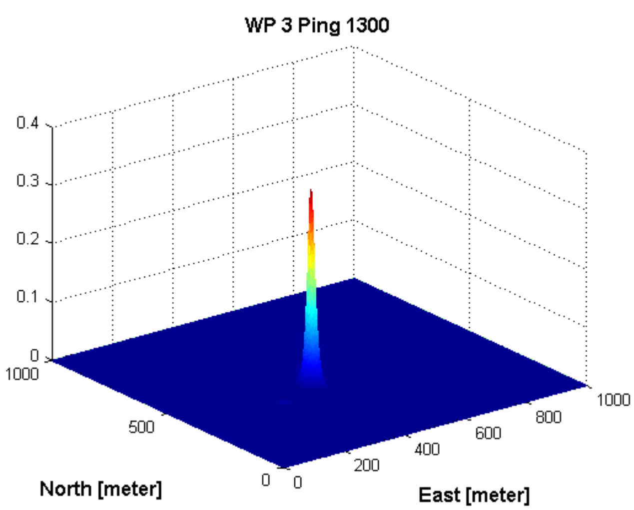

Fig. 17. Likelihood function for ping 1300.

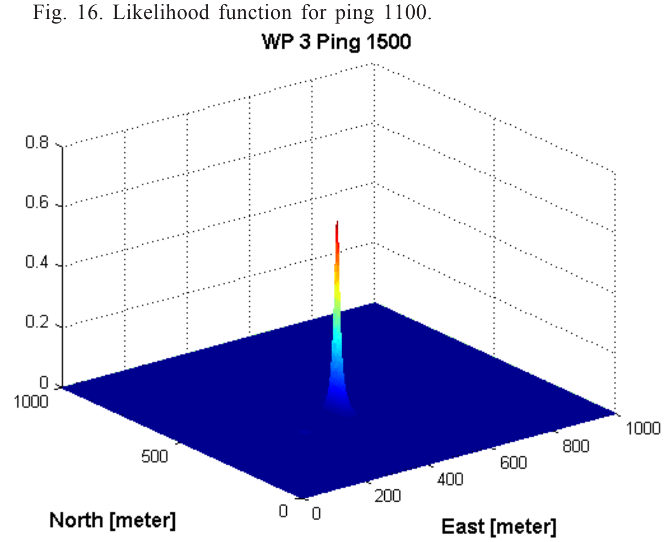

Fig. 18. Likelihood function for ping 1500.

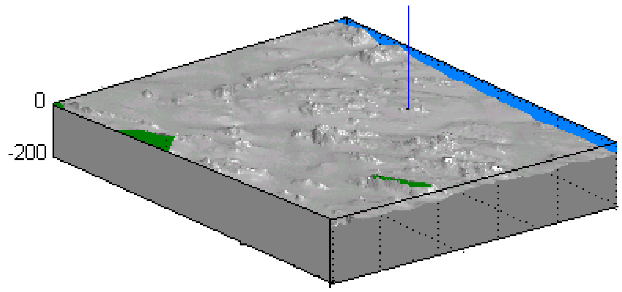

Fig. 19. Underwater map over a 5 x 5 km large area. The vertical pole indicates a pre-selected way-point. Note the difference in vertical and horizontal scale.

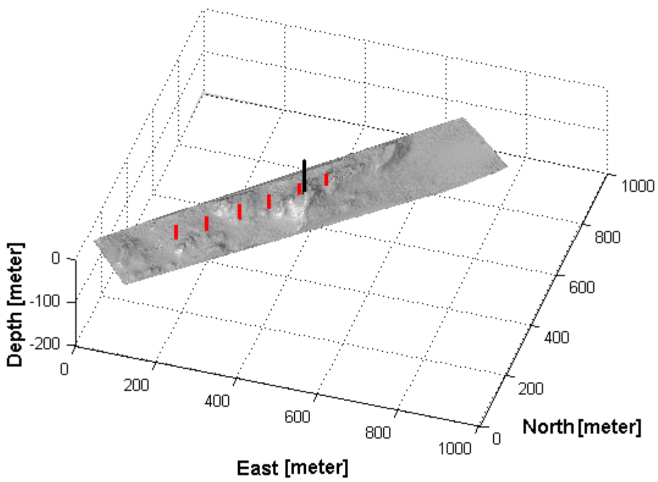

Fig. 20. Way-point 3. Different correlation points (red). The black pole indicates the pre-selected way-point.

It should be noted that the DGPS's RMS position error is in the 2 -3 meter range and that it is included in the figures in Table II. So is also the horizontal map random error of approximately 1 – 2 meters. The actual position error due to the correlation method is thus much less than the figures in Table II.

VII. CONCLUSIONS

It has been shown that using a sonar with many

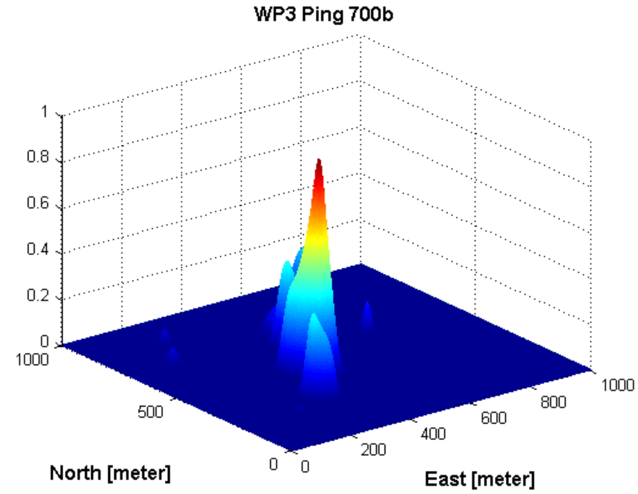

Fig. 21. Likelihood function for ping 700. The bottom area is 97 meter x 102 meter.

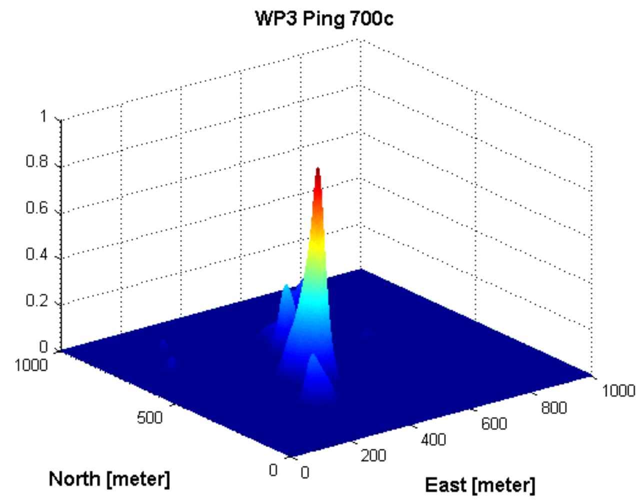

Fig. 22. Likelihood function for ping 700. The bottom area is 121 meter x 102 meter.

measurement beams will considerably increase both accuracy and robustness in terrain navigation. The position can in many cases be determined without a prior PDF for the position.

It has also been shown that a linear Kalman filter with

Table I. Position error relative the DGPS-measurement.

Error	Ping 500	Ping 700	Ping 900	Ping 1100	Ping 1300	Ping 1500
East meter	-10.5	-, -5.8, -7.1	-8.1	-8.9	-0.7	-5.4
North meter	-10.6	-, -12.9, -15.4	-15.2	-12.4	-7.1	-6.4

Table II. Mean reduced position error of the values from Table I, including DGPS-error.

Error	Ping 500	Ping 700	Ping 900	Ping 1100	Ping 1300	Ping 1500
East meter	-3.8	0.8	-1.5	-2.3	5.9	1.2
North meter	-0.8	-1.5	-3.8	-1.0	4.3	5.0
Circular meter	3.9	1.7	4.0	2.5	7.4	5.2

almost optimal performance can be used if many measurement beams are used. This makes it easy to add states for handling the biases in the INS-system.

Acknowledgment

The authors would like to thank Mr. Carl-Johan Andersson and CDR. Stefan Ahlberg at The Material Administration, FMV, Sweden for their financial support of this research project.

Thanks are also due to the Reson Company and Technical Director T. Meurling, MSc., and Sales Manager Navy C. W. Glädesdahl, MSc., and Hydrographer R. Hill, BSc., for their kind support during the sea trial. Reson personnel collected the bathymetric data during the sea trial.

References

[1] L. D. Hostetler, R. D. Andreas,"Nonlinear Kalman Filtering Techniques for Terrain-Aided Navigation" in H.W. Sorensen, editor, *Kalman filtering: Theory and Application,* IEEE Press 1985.

[2] A. J. Robins, "Recent Developments in the TERPROM Integrated Navigation System", Proceedings of the 44th Annual ION Meeting. Annapolis, Maryland. June 1988.

[3] O. Bergem, "Bathymetric Navigation of Autonomous Underwater Vehicles using a Multibeam Sonar and a Kalman Filter with Relative Measurement Covariance Matrices", Dr. Scient thesis, University of Trondheim, Norway, 1993.

[4] N. Bergman, "Recursive Bayesian Estimation, Navigation and Tracking Applications", PhD thesis, Department of Electrical Engineering, Linköping University, Linköping, Sweden, 1999.

[5] I. Nygren, "A Method for Terrain Navigation of an AUV", Conference proceedings, MTS/IEEE Oceans 2001.

[6] S. M. Kay, *Fundamentals of Statistical Signal Processing, Estimation Theory*, Prentice Hall 1993.

[7] H. L. Van Trees, *Detection, Estimation and Modulation Theory*. Wiley, New York,1968.

[8] R. G. Brown, P. Y. C. Hwang, *Introduction to Random Signals and Applied Kalman Filtering*, John Wiley & Sons 1997.

[9] F. Gustavsson, F. Gunnarsson, N. Bergman, U. Forssell, J. Jansson, R. Karlsson, P.-J. Nordlund, "Particle Filters for Positioning, Navigation, and Tracking". IEEE Transactions on Signal Processing, Vol. 50, No 2, 2002.

[10] K. Murphy, S. Russel,"Rao-Blackwellised Particle Filtering for Dynamic Bayesian Networks" in A. Doucet, N. de Freitas, Neil Gordon, editors, *Sequential Monte Carlo Methods in Practice*, Springer 2001.

[11] K. Andersson, F. Traugott, "Implementation of a Terrain Correlator for an Underwater Vehicle in an FPGA", Master